*Am. J. Hum. Genet. 63:415–427, 1998*

# Exhaustive Screening of the Acid β-Glucosidase Gene, by Fluorescence-Assisted Mismatch Analysis Using Universal Primers: Mutation Profile and Genotype/Phenotype Correlations in Gaucher Disease

Dominique P. Germain,[1,2] Jean-Philippe Puech,[1] Catherine Caillaud,[1,2] Axel Kahn,[2] and Livia Poenaru[1,2]

[1]Laboratoire de Génétique et Pathologie Métabolique and [2]Institut National de la Santé et de la Recherche Médicale (INSERM) U.129, Institut Cochin de Génétique Moléculaire (ICGM), Hôpital Cochin, Université René Descartes, Paris

## Summary

**Gaucher disease (GD) is one of the most prevalent lysosomal storage disorders and one of the rare genetic diseases now accessible to therapy. Outside the Ashkenazi Jewish community, a high molecular diversity is observed, leaving ~30% of alleles undetected. Nevertheless, very few exhaustive methods have been developed for extensive gene screening of a large series of patients. Our approach for a complete search of mutations was the association of fluorescent chemical cleavage of mismatches with a universal strand-specific labeling system. The glucocerebrosidase (*GBA*) gene was scanned by use of a set of six amplicons, comprising 11 exons, all exon/intron boundaries, and the promoter region. By use of this screening strategy, the difficulties due to the existence of a highly homologous pseudogene were easily overcome, and both GD mutant alleles were identified in all 25 patients studied, thus attesting to a sensitivity that approaches 100%. A total of 18 different mutations and a new glucocerebrosidase haplotype were detected. The mutational spectrum included eight novel acid β-glucosidase mutations: IVS2 G(+1)→T, I119T, R170P, N188K, S237P, K303I, L324P, and A446P. These data further indicate the genetic heterogeneity of the lesions causing GD. Established genotype/phenotype correlations generally were confirmed, but notable disparities were disclosed in several cases, thus underlining the limitation in the prognostic value of genotyping. The observed influence of multifactorial control on this monogenic disease is discussed.**

Received March 2, 1998; accepted for publication May 26, 1998; electronically published July 10, 1998.

Address for correspondence and reprints: Dr. Dominique P. Germain, INSERM U.129, CHU Cochin Port-Royal, 24 rue du Faubourg Saint Jacques, 75014 Paris, France. E-mail: germain@cochin.inserm.fr


0002-9297/98/6302-0017$02.00

## Introduction

Gaucher disease (GD), the most frequent lysosomal storage disorder, is an autosomal recessive disease characterized by deficiency of acid β-glucosidase (glucocerebrosidase, E.C.3.2.1.45) (Beutler and Grabowski 1995; Grabowski et al. 1996). The enzymatic defect leads to systemic accumulation of its substrate, glucosylceramide (also named "glucocerebroside"), mainly within cells of the monocyte/macrophage lineage, resulting in the clinical manifestations. GD, characterized by a large and continually expanding phenotypic heterogeneity (Sidransky and Ginns 1993; Abrahamov et al. 1995), conventionally is classified into three clinical types, on the basis of the absence (type 1) or presence and severity (types 2 and 3) of primary CNS involvement. Type 1 GD (MIM 230800) is the most common form, with a markedly heterogeneous clinical expression, with respect to age at onset, progression, and severity of clinical manifestations. Common features are splenomegaly, frequent concurrent liver enlargement, and consequent anemia and thrombocytopenia. In severe cases, orthopedic complications occur. The much rarer clinical types, 2 (MIM 230900) and 3 (MIM 231000), differ from type 1 in that patients show neurological involvement; type 2 usually manifests soon after birth, whereas type 3 may appear as late as the 3d decade of life (Brady et al. 1993). The full-length cDNA and genomic sequences encoding human glucocerebrosidase have been isolated and characterized (Sorje et al. 1985; Horowitz et al. 1989; Beutler et al. 1992). The active gene (*GBA*), localized to the long arm of chromosome 1 at 1q21, contains 11 exons spanning 8 kb. A highly homologous pseudogene (*psGBA*), transcribable into mRNA but unable to produce a functional enzyme, is located 16 kb downstream from the active gene (Horowitz et al. 1989). Cloning of the *GBA* gene has allowed identification of the nature of mutations underlying the enzyme deficiency in GD patients. Various studies have demonstrated the molecular heterogeneity of acid β-glucosidase deficiency. More than 70 gene alterations responsible for the disease have

been identified (Beutler and Gelbart 1996). The relative incidence of glucocerebrosidase mutations has been studied extensively in the Ashkenazi Jewish population(s), in which four defects (N370S, 84insG, L444P, and IVS2 G[+1]→A) account for 90% of the disease-causing changes (Beutler et al. 1993). A more heterogeneous distribution of mutations within the non-Jewish population(s) has emerged, and mutation frequencies in defined populations have been reported in recent studies (Amaral et al. 1994; Cormand et al. 1995; Boot et al. 1997; Le Coutre et al. 1997). However, all these studies have focused on common mutations, leaving ~30% of the alleles undetected in non-Jewish populations.

Two main reasons may justify a full investigation of mutations. First, identification of novel mutations may prove useful for genetic counseling and prenatal diagnosis in families in which these mutations are found (Zimran et al. 1995), since enzymology does not provide accurate carrier detection (Daniel and Glew 1982); second, such an investigation may help to further delineate genotype/phenotype correlations and disparities.

Very few exhaustive mutational analyses of the *GBA* gene have been reported; many authors deliberately chose to scan only a limited number of exons and/or mentioned a lack of sensitivity that is hardly acceptable in a medical context. Chemical cleavage of mismatches (CCM), based on cleavage of heteroduplex DNA at mispaired bases and sizing of the truncated DNA strands, has proved effective in the screening of large DNA regions (Cotton et al. 1988). The possibility of analyzing large fragments allows more flexibility in the design of primers. Adaptation to fluorescence-based detection systems, through a nested PCR, in a procedure named "fluorescence-assisted mismatch analysis" ("FAMA") has simplified the method and has maximized positional precision and diagnostic accuracy (Verpy et al. 1994; Germain et al. 1996). However, the high cost of producing new, fluorescently tagged specific primers for each of the amplicons prompted us to design and develop a single, universal priming system for the highly specific fluorescent labeling of DNA-amplification products (fig. 1). In this study, we demonstrated the advantages of this universal strand-specific bifluorescent-labeling strategy combined with CCM, by completing an exhaustive mutation detection in 25 GD patients. Eight novel mutations and a new *GBA* haplotype are described, genotype/phenotype correlations and disparities are delineated, and the influence of multifactorial factors is discussed.

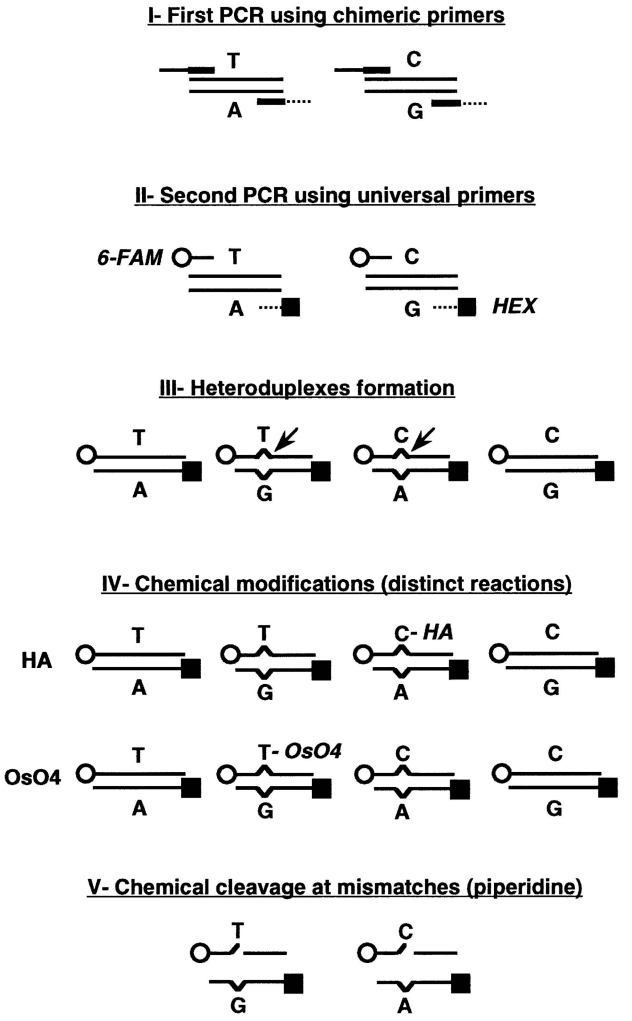


**Figure 1** Principle of the FAMA method using universal fluorescent primers. For each region, the first PCR is performed by use of long-tailed primers consisting of two portions: the 3′ half has the necessary homology for a specific amplification of the acid β-glucosidase functional gene, and the 5′ half has been chosen for minimal homology to any sequence in human-genome databases (*part I*) and will serve as a universal template for the second step of amplification with primers labeled, at their 5′ ends, with different fluorophores (6-FAM and HEX for the sense and the antisense strand, respectively) (*part II*). In the case shown (*part III*), the heterozygous C→T transition gives rise to two heteroduplex mismatches (C-A and T-G). By means of chemical modifications by HA and osmium tetroxide, which react with mispaired cytosines and thymines, respectively (*part IV*), cleavage with piperidine ensures detection of two cleavage products for each point mutation and maximizes precision in the positioning of the sequence heterogeneity (*part V*). In the illustrated example, a cleavage peak will be detected on the sense strand, at the same location, for each modification reaction (HA and osmium tetroxide chemistries).

## Patients and Methods

### *Patients*

The 25 unrelated patients (10 females and 15 males; 4–73 years of age) in this study were diagnosed by clinical examination and by determination of 4-methyl umbelliferyl-β-glucosidase activity in leukocytes. The physicians who contributed patient blood samples to our study provided clinical information concerning their pa-

tients. The results of examinations of our patients have not been published previously. The geographic origin of the patients is spread throughout different regions in France; therefore, this group's panel can be considered to be representative of the French population.

### *Amplification of Genomic DNA Fragments, by Use of a Universal Fluorescent-Labeling System*

Genomic DNA for mutation analysis was prepared from peripheral blood leukocytes or lymphoblastoid cell lines by standard procedures. Six fragments covering the acid $\beta$-glucosidase gene were amplified (fig. 2). For each region, 500 ng of genomic DNA was used for a first round of PCR amplification, using the unlabeled chimeric oligonucleotide primers listed in table 1. These primers were chosen to specifically amplify the active gene and not the pseudogene and were extended by universal sequences at their 5′ ends. Since this labeling strategy requires that the first PCR be free of spurious amplification products, high specificity was obtained by priming at sites with a particularly rare sequence composition. This was achieved by choosing rare sequences for the 3′ end of each nonfluorescent primer in human-genome databases (Griffais et al. 1991). PCR products were checked on a 1% agarose gel, and a 1/100 dilution was submitted to a second round of PCR, using the universal primers complementary to the universal extensions of the chimeric primers, labeled at their 5′ ends with 6-carboxyfluoresceine (for the forward primer) and hexachlorofluoresceine (for the reverse primer) fluorescent dyes (fig. 1). These universal primers were designed, by use of PC-Rare software, to have a unique sequence exhibiting minimal homology to any sequence found in current human–DNA-sequence databases (Griffais et al. 1991).

### *Fluorescent CCM*

Heteroduplexes were made from a normal control and from the patients' labeled DNA, by boiling—for 5 min in 200 $\mu$l of 0.3 M NaCl, 3.5 mM $MgCl_2$, and 3 mM Tris-HCl, pH 7.7—1 pmol of bichrome PCR fragments, which then were placed in a water bath at 65°C overnight. The heteroduplexes were ethanol precipitated after addition of 60 $\mu$g glycogen (Boehringer) as a carrier and were resuspended in 24 $\mu$l distilled water (or in 10 mM Tris HCl, pH 7.5). Modification reactions then were performed by incubating 6 $\mu$l of DNA, at 37°C for 45 min, with 20 $\mu$l of a freshly thawed 3.8-M hydroxylamine (HA) working solution, whereas another aliquot of 6 $\mu$l was treated, for 15 min at room temperature, with 9 $\mu$l of reaction buffer (6.94% pyridine, 1.388 mM $Na_2EDTA$, and 13.88 mM Hepes, pH 8.0) and 10 $\mu$l of 1% osmium tetroxide, in a total volume of 25 $\mu$l in silanized tubes (aliquots of both the HA working solution and the 1% osmium tetroxide stock solution were stored at −80°C for up to 6 mo, thus removing potential hazards associated with repeated preparation). The modification reactions were blocked by adding 200 $\mu$l of ice-cold stop solution (0.3 M sodium acetate, pH 5.2, and 0.1 mM $Na_2EDTA$), and the nucleic acids were ethanol precipitated in a dry ice/ethanol bath. Pellets were washed once with 70% ethanol, resuspended by vortexing in 50 $\mu$l of freshly diluted 1-M piperidine, and incubated 20 min at 90°C. The nucleic acids were precipitated, washed twice in 70% ethanol, vacuum dried, and, when necessary, stored at −20°C until loading. Pel-

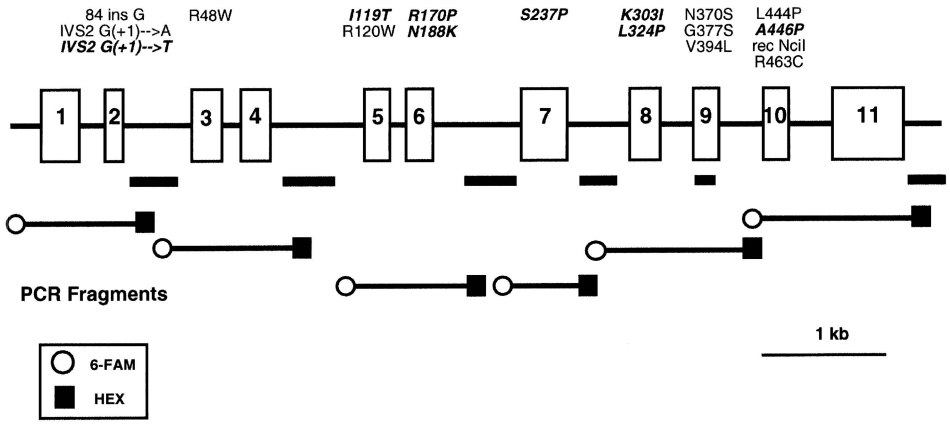


**Figure 2** Screening strategy and distribution of mutations identified in this report. The structure of the acid $\beta$-glucosidase gene is shown, with exons represented by boxes and introns represented by lines. Blackened bars beneath the gene indicate the regions with absence of homology with the pseudogene. PCR-amplified fragments are represented with their terminal fluorophores, 6-FAM (*circles*) or HEX (*squares*), at the bottom of the figure. The locations of all mutations identified in this report are shown above the schematic diagram of the gene. The novel mutations are indicated in boldface, italic type.

**Table 1**

**Parameters for Amplification of the Acid β-Glucosidase Gene Fragments**

| Exon(s) and/or Fragment | Primer Sequence (5′→3′)[a] | Acid β-Glucosidase Gene Coordinates | Size of Amplified Product (bp) |
|---|---|---|---|
| First PCR: | | | |
| 1 and 2: | | | |
| Forward | ggACCgTTAgTAACCgAC-CACACCTCTATAGGGCAAAGACTG | 75–98 | 1,266 |
| Reverse | AgTCggATAgCTAgTCgT-GAGGCAGAGGTTGGAATGAGCCAA | 1282–1305 | |
| 3 and 4: | | | |
| Forward | ggACCgTTAgTAACCgAC-AACAgAgTCTTACTCTgTTgCCTggg | 1235–1260 | 1,066 |
| Reverse | TCggATAgCTAgTCgT-TgAggCAggAgAATCACTATAgCC | 2242–2265 | |
| 5 and 6: | | | |
| Forward | ggACCgTTAgTAACCgAC-ACTATTAGGACTGGCAAGTG | 2961–2980 | 931 |
| Reverse | TCggATAgCTAgTCgT-TACAGTGAGTGAAGATGGCG | 3837–3856 | |
| 7: | | | |
| Forward | ggACCgTTAgTAACCgAC-GGGTTTCGCCAGGCTGTTCTCG | 3967–3988 | 882 |
| Reverse | AgTCggATAgCTAgTCgT-GAGATGGAGTCTCGCTCAGCCT | 4792–4813 | |
| 8 and 9: | | | |
| Forward | ggACCgTTAgTAACCgAC-AAATTAGCTGGGTGTGGCACCCGT | 4944–4967 | 1,268 |
| Reverse | AgTCggATAgCTAgTCgT-GTCACTTCCTGCCTCCATGGTGCA | 6153–6176 | |
| 10 and 11: | | | |
| Forward | ggACCgTTAgTAACCgAC-TGGGGTGGGTCCGTGGGTGG | 6296–6315 | 1,191 |
| Reverse | AgTCggATAgCTAgTCgT-GTCTCCATCCAGCGGGCAAC | 7432–7451 | |
| Second PCR: | | | |
| Forward | 6-FAM-ggggACCgTTAgTAACCgAC | Universal primer | |
| Reverse | HEX-ggAgTCggATAgCTAgTCgT | Universal primer | |

[a] Universal extensions and primers are underlined.

lets were dissolved in a solution of 6 μl deionized formamide and 50 mM $Na_2EDTA$, and 3 μl of each sample, mixed with 0.5 μl of fluorescence-labeled size standard (GS2500 ROX; ABI), was heated to 95°C for 5 min and kept on ice until loading on a 6% polyacrylamide/urea gel on an automated ABI 373 DNA sequencer. Electrophoresis was performed overnight for up to 20 h in 1 × Tris borate–EDTA, at 35 W, and data were collected and analyzed by use of the appropriate GENESCAN software (ABI). For a sizing requirement of the software, the 3′ ends of nonfluorescent primers were positioned directly at a distance of ⩾70 bp from the target sequence.

### *Sequencing*

When cleavage peaks were encountered in FAMA, independently PCR-amplified fragments of the corresponding region were sequenced on both strands, to determine the precise nature of the mutation. PCR products were purified by use of the QIAquick Spin PCR purification kit (Qiagen), to remove unincorporated oligonucleotide primers. All sequencing reactions were performed on an automated ABI 373A DNA sequencer with the Prism DyeDeoxy Terminator sequencing kit (ABI), in accordance with the manufacturer's recommendations.

### *Nomenclature*

The designations for the mutations refer to the position of the amino acid substitution, where amino acid 1 is the amino terminus of the mature protein. The cDNA base numbers refer to the position of the nucleotide in the cDNA, where nucleotide 1 is the A of the first ATG (Genbank/European Molecular Biology Laboratory [EMBL] accession number M11080). The genomic designations are based on the updated acid β-glucosidase Genbank/EMBL sequence (accession number J03059), from which the first 875 nucleotides in the 5′ UTR have been deleted. The first nucleotide of exon 1 is at genomic position 355 (Grace et al. 1997).

## Results

### *Clinical Forms and Geographic Distribution of Affected Patients*

Clinical symptoms, β-glucosidase activities, and genotypes of all patients are presented in table 2. All 25 unrelated patients are of French origin, and only two of them (patients 1 and 10) are of Ashkenazi Jewish descent. At the time of the study, only two patients had developed neurological symptoms, establishing that they had type 3 GD. Since one patient without neurological symptoms was <15 years of age, final classification (type

## Table 2

**Clinical Characteristics of Patients with Associated Genotypes**

| Patient (Initials) | Present Age/Age at Diagnosis (years) | Sex | Clinical Signs (Treatment) | Neuronopathy | GD Clinical Type | 4−Methyl Umbelliferyl-β-Glucosidase Activity[a] | Genotype |
|---|---|---|---|---|---|---|---|
| 1 (MS) | 67/29 | M | Splenomegaly (splenectomy), osteosarcoma | None | 1 | 9 | N370S/84insG |
| 2 (CB) | 53/9 | F | Severe hepatosplenomegaly (splenectomy), anemia, skeletal deterioration | None | 1 | 4 | N370S/IVS2 G(+1)→T |
| 3 (PL) | 33/5 | M | Hepatosplenomegaly, severe pancytopenia | None | 1 | 15 | N370S/I119T |
| 4 (MF) | 68/65 | F | Mild splenomegaly, mild thrombocytopenia | None | 1 | 7 | N370S/R120W |
| 5 (MCL) | 50/35 | F | Moderate splenomegaly, mild hepatomegaly, thrombocytopenia | None | 1 | ? | N370S/R120W |
| 6 (SL) | 26/22 | M | Pancytopenia, severe skeletal disease | None | 1 | 4 | N370S/R120W |
| 7 (CN) | 27/25 | M | Splenomegaly (splenectomy), hepatomegaly, thrombocytopenia, pain | None | 1 | 6 | N370S/N188K |
| 8 (BC) | 14/4 | M | Massive splenomegaly, hepatomegaly, skeletal deterioration | None | 1 | 17 | N370S/S237P |
| 9 (CG) | 34/30 | M | Massive splenomegaly | None | 1 | 2 | N370S/L324P |
| 10 (GM) | 73/65 | M | Mild splenomegaly, hepatomegaly, thrombocytopenia | None | 1 | 18 | N370S/N370S |
| 11 (VF) | 26/15 | F | Mild splenomegaly | None | 1 | 18 | N370S/N370S |
| 12 (MD) | ?/? | F | Unknown | None | 1 | ? | N370S/G377S |
| 13 (GS) | 24/? | F | Hepatosplenomegaly, bone crises, skeletal deterioration | None | 1 | 10 | N370S/rec NciI |
| 14 (FF) | 28/23 | M | Mild hepatosplenomegaly, no skeletal complications | None | 1 | 6 | N370S/L444P[b] |
| 15 (JG) | 54/45 | M | Splenomegaly, hepatomegaly, thrombocytopenia, massive osteopathy | None | 1 | 6 | N370S/L444P[b] |
| 16 (JP) | 22/3 | M | Massive splenomegaly, thrombocytopenia, skeletal pain | None | 1 | 5 | N370S/L444P[b] |
| 17 (IA) | 32/27 | F | Splenomegaly, mild pancytopenia | None | 1 | 9 | L444P/R48W |
| 18 (YD) | 4/1 | M | Massive hepatosplenomegaly | Abnormal eye movements | 1/3 | 16 | L444P/L444P[b] |
| 19 (AP) | 10/1 | F | Massive hepatosplenomegaly | Strabismus, modified EEG | 3 | 18 | L444P/L444P[b] |
| 20 (JG) | 36/31 | M | Mild symptomatology | None | 1 | 15 | L444P/R463C |
| 21 (ES) | 6 (deceased)/1 | M | Splenomegaly, thrombocytopenia, deceased at 6 years of age despite enzyme recombinant therapy | Ataxia, epilepsy | 3 | 0 | rec NciI/V394L |
| 22 (AP) | 62/59 | M | Mild symptomatology | None | 1 | 16 | R463C/K303I |

(*continued*)

**Table 2 (continued)**

| Patient (Initials) | Present Age/Age at Diagnosis (years) | Sex | Clinical Signs (Treatment) | Neuronopathy | GD Clinical Type | 4−Methyl Umbelliferyl-β-Glucosidase Activity[a] | Genotype |
|---|---|---|---|---|---|---|---|
| 23 (BS) | 19/? | M | Hepatosplenomegaly, bone crises, skin pigmentation | None | 1 | 13 | IVS2 G(+1)→A/R170P |
| 24 (ML) | 49/49 | F | Massive splenomegaly | None | 1 | 19 | G377S/G377S |
| 25a (VT) | 31/10 | F | Splenomegaly (splenectomy), severe skeletal deterioration, confined to wheelchair | None | 1 | 8 | A446P/A446P |
| 25b (GT)[c] | 29/? | M | Asymptomatic | None | 1 | 20 | A446P/A446P |

[a] Residual enzymatic activities are expressed as the percentage of control values.
[b] Complex alleles were ruled out.
[c] Brother of patient 25a.

1 or type 3 GD) had to be postponed. The remaining patients presented with type 1 GD.

### *Identification of Unknown Mutations, by FAMA Using Universal Primers*

The 7.6-kb β-glucosidase gene was amplified in six DNA fragments spanning the whole coding region, all exon-intron boundaries, the 200 bp 5′ to the transcription start site, and 700 bp of the 3′ noncoding region (fig. 2). No size abnormality was detected when amplified products were analyzed by agarose-gel electrophoresis. For all patients, the six bichrome PCR fragments, shown in figure 2, were studied by fluorescent CCM (i.e., FAMA). Direct sequencing of the relevant region was used to formally verify all detected mutations. This exhaustive screening of the acid β-glucosidase gene resulted in characterization of the genotypes of all 25 patients (table 2) and identification of eight novel point mutations (IVS2 G[+1]→T, I119T, R170P, N188K, S237P, K303I, L324P, and A446P; fig. 2). Other alleles found included the three common mutations N370S, L444P, and 84insG, as well as two frequent glucocerebrosidase mutant alleles (IVS2 G[+1]→A and the complex allele rec NciI [L444P + A456P + V460V]). The frequent D409H mutation (Abrahamov et al. 1995) was not evidenced in our series. We also detected five rare, previously reported mutations (R48W, R120W, G377S, V394L, and R463C). The identified nucleotide substitutions and the resulting changes at the protein level are presented in table 3.

Some of the characterized genotypes were of particular interest. One recurrent genotype was found in three unrelated patients originating from the same area of France, namely, Brittany. Screening of patients 4, 5, and 6 demonstrated that they are compound heterozygotes for the common N370S allele. Unexpectedly, FAMA of these three patients also revealed the same C→T transition in exon 5 (fig. 3), changing an arginine (CGG) to tryptophan (TGG) at position 120 of the mature enzyme (R120W). Notably, the mutation destroys an *Msp*I restriction site, which can be used as a screening strategy. The surrounding sequence was not that of the pseudogene (fig. 3) and, therefore, not the product of an extensive unequal crossover, as had been reported elsewhere (Latham et al. 1991).

Patient 7 also was a compound heterozygote for the N370S mutation, with his second allele carrying a T→G transversion in exon 6, at position 3482 (N188K) in the genomic sequence. This nucleotide substitution corresponds to the pseudogene sequence at the analogous site and also has been reported to be part of the aforementioned complex allele (Latham et al. 1991). However, in the case of our patient, a crossover event between the structural gene and the pseudogene was not likely, since other pseudogene-like substitutions at contiguous sites were not present. These data were formally controlled by direct sequencing.

Analysis, by FAMA, of the *GBA* gene in patient 21 showed a complex allele, thus illustrating the possibility of using this technique to detect multiple sequence changes in large DNA fragments (fig. 4). This complex allele, named "rec NciI," consists of a single-base substitution in three different codons: codon 444, Leu (C<u>T</u>G)→Pro (C<u>C</u>G); codon 456, Ala (<u>G</u>CT)→Pro (<u>C</u>CT); and codon 460, Val (GT<u>G</u>)→Val (GT<u>C</u>) (Latham et al. 1990). This mutant allele is identical in sequence to a region of the pseudogene (Horowitz et al. 1989) and may be the result of a fusion gene or a gene conversion. This severely affected type 3 GD patient died at 6 years of age, despite prolonged enzyme recombinant therapy that improved the visceral manifestations but not the neurological ones; his second allele was shown to carry

**Table 3**

**Novel Mutations Identified in Patients with GD**

| Patient(s) | Designation | cDNA Position | Genomic Position | Codon Change | Exon or Intron | Amino Acid Change |
|---|---|---|---|---|---|---|
| 2 | IVS2 G(+1)→T | ... | 1067 | ... | Intron 2 | Splice (AGgt→AGtt) |
| 3 | I119T | 473 | 3064 | ATC→ACC | Exon 5 | Isoleucine119→threonine |
| 23 | R170P | 626 | 3427 | CGT→CCT | Exon 6 | Arginine170→proline |
| 7 | N188K | 681 | 3482 | AAT→AAG | Exon 6 | Asparagine188→lysine |
| 8 | S237P | 826 | 4182 | TCT→CCT | Exon 7 | Serine237→proline |
| 22 | K303I | 1025 | 5252 | AAA→ATA | Exon 8 | Lysine303→isoleucine |
| 9 | L324P | 1088 | 5315 | CTA→CCA | Exon 8 | Leucine324→proline |
| 25a, 25b | A446P | 1453 | 6449 | GCA→CCA | Exon 10 | Alanine446→proline |

a G→T transversion at position 5924, resulting in a Val→Leu substitution at codon 394 of the mature enzyme.

Patient 25a, suffering from a severe type 1 GD, and her very mildly affected brother presented with striking phenotypic differences. In both of them, a G→C transversion was revealed at position 6449 in exon 10 of the structural gene, predicting an A446P missense mutation at the protein level. Despite complete mutation scanning of the rest of the gene, no other sequence abnormality was found. In fact, the presence of a normal A446 allele was excluded in an additional investigation, without addition of normal control DNA, which failed to reveal the aforementioned cleavage peak. This strongly suggested either a deletion of the other *GBA* allele or homozygosity for the A446P mutation (Dianzani et al. 1991). Further inquiries revealed that these patients were the offspring of a consanguineous couple, and sequencing of the relevant $\beta$-glucosidase–gene region in the parents confirmed that both were heteroallelic for A446P.

A mutation (IVS2 G[+1]→T) was identified at the consensus donor splice site of intron 2, when the *GBA* gene in patient 2 was analyzed. This novel mutation differs from the already described IVS2 G(+1)→A allele, which is thought to arise from genetic recombination with the pseudogene (He and Grabowski 1992). The second allele was shown, by FAMA, to be the N370S common mutation. During this latter mutation search, another sequence heterogeneity unexpectedly was evidenced simultaneously in intron 7 (data not shown). This heteroallelism actually corresponded to a polymorphism. Several other intragenic polymorphic sites (RFLPs) were investigated subsequently by genomic sequencing or restriction cleavage. This led us to document the existence of a novel *GBA* haplotype, which has been identified by 6 of the 12 initially described RFLPs. This variant was found again in another French patient (patient 17), who carried a different genotype (R48W/L444P).

## Discussion

The aim of the present survey was to determine the precise nature and distribution of mutations in 25 GD patients and to document the efficiency of FAMA by chemical cleavage, combined with a new universal priming system, to screen for unknown mutations.

### *Screening Strategy*

Comparisons of different DNA scanning methods should provide indications as to the best choice(s) in a diagnostic context (Grompe 1993; Cotton 1997). Several PCR-based technologies have been used for the screening of the *GBA* gene, thereby contributing to the determination of the frequency of recurrent mutations. Nevertheless, the majority of the studies using these methods focused on the most common mutations (N370S, L444P, and 84insG), resulting in ~30% undetected alleles in non-Jewish populations. The most complete approaches have used SSCP combined with nested PCR (Sibille et al. 1993) and, more recently, long PCR (Tayebi et al. 1996). However, very few exhaustive screenings, for unknown mutations, of the complete gene in a large series of patients have been performed by use of these methods, and most authors report a lack of sensitivity in their screening strategy.

Our approach was to develop an exhaustive screening method by combining CCM with a universal strand-specific fluorescent-labeling system. CCM is a powerful technique with sensitivity approaching 100% (Cotton et al. 1988). Its potential toxicity was reduced by storage of both HA and osmium tetroxide in aliquots kept at −80°C and by fluorescence labeling of the DNA fragments. Strand-specific fluorescent labeling offers significant improvements in identification and localization of mismatches (Verpy et al. 1994; Rowley et al. 1995; Germain et al. 1996). An absolute requirement was to distinguish between the *GBA* gene and the pseudogene. This was achieved by amplification of large DNA fragments, which gives more flexibility in the design of primers (fig. 2).

Differential DNA-strand fluorescent labeling classically has been performed by a nested PCR, by use of region-specific fluorescent primers. However, producing new, fluorescently tagged primers for each of the amplicons studied is costly. Moreover, nested PCR requires

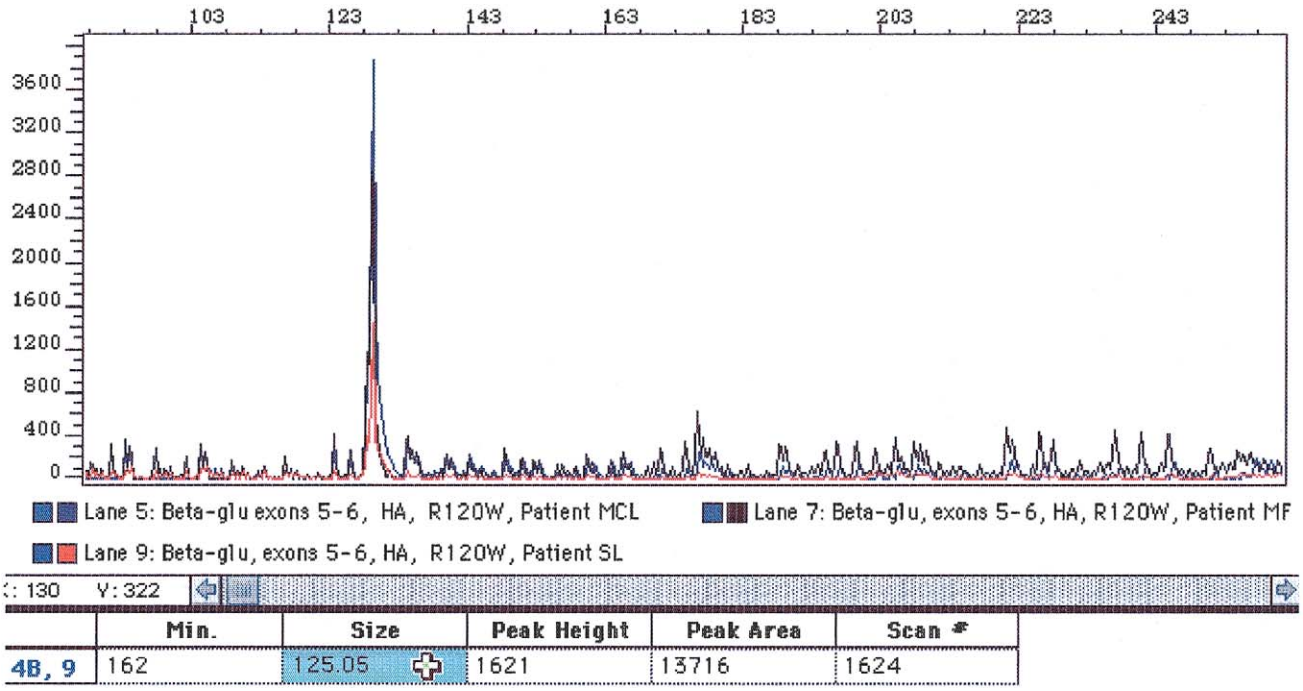


**Figure 3** Detection of missense point mutation R120W. This C→T transition was found in exon 5 in three unrelated patients (4, 5, and 6). The three fluorescence profiles of the sense strand—indicated here, for convenience, in blue, black, and red—are perfectly superimposed. This C→T transition gives rise to two different heteroduplexes (C-A and T-G). By means of HA modification and piperidine cleavage, the C-A mismatch is precisely localized, by the software (as shown by the cross in the table), at a position 125 bp from the 5′ terminal fluorescent label. Analysis of cleavage signals of very low amplitude, at surrounding sequences, reflects weak but specific modifications at each paired C residue, thus improving precision in the positioning of the mutation and allowing coamplification of *psGBA* sequences to be ruled out. Osmium tetroxide chemistry yielded similar results for the T-G mismatch (not shown).

optimization of yield and quality of the second PCR; we therefore devised a universal priming strategy to circumvent both these aspects (fig. 1). High specificity of amplification was obtained by choosing rare sequences for the 3′ ends of the nonfluorescent primers and by designing each of the two "universal" extensions to have minimal homology to any sequence found in human–DNA-sequence databases (Griffais et al. 1991).

Once PCR conditions were determined, the FAMA method allowed an exhaustive molecular diagnosis of the *GBA* gene, with a sensitivity approaching 100%, since all 50 mutant alleles of the 25 patients were characterized. Conversely, in spite of constant improvements of sequencing chemistries, direct automated sequencing does not guarantee complete detection of heterozygous mutations and requires time-consuming and costly optimizations (Kwok et al. 1994), which are not yet suited to diagnostic tasks (Phelps et al. 1995; Verpy et al. 1996).

### *Mutation Profile and Haplotype Analysis*

Among the 50 alleles studied, 32 (64%) carried the recurrent mutations N370S, L444P, and 84insG, accounting for 19, 12, and 1 allele(s), respectively. Data concerning the N370S mutation differ from those from initial investigations of non-Jewish patients (Beutler and Gelbart 1993) but agree with frequencies reported for other European populations (Cormand et al. 1995; Le Coutre et al. 1997). Thus, the N370S mutation, which has not been evidenced in a large Japanese series (Ida et al. 1995), appears to be common in all European populations and possibly may have been enriched within the Ashkenazi community by endogamy. The observed frequency of the L444P mutation (24%) is lower than that observed in America (Beutler and Gelbart 1993), Israel (Horowitz et al. 1993), or Asia (Ida et al. 1995) but is in accordance with results from other studies of European populations (Boot et al. 1997; Le Coutre et al. 1997); no data were available from Africa. The 84insG mutation was found only in one patient of Ashkenazi Jewish extraction, further corroborating the ethnic specificity of this allele.

A second group included seven previously reported mutant alleles (IVS2 G[+1]→A, R48W, R120W, G377S, V394L, R463C, and rec NciI) (Beutler and Gelbart 1996). All of them were found in single cases, except for R463C, which was found twice, and R120W, which

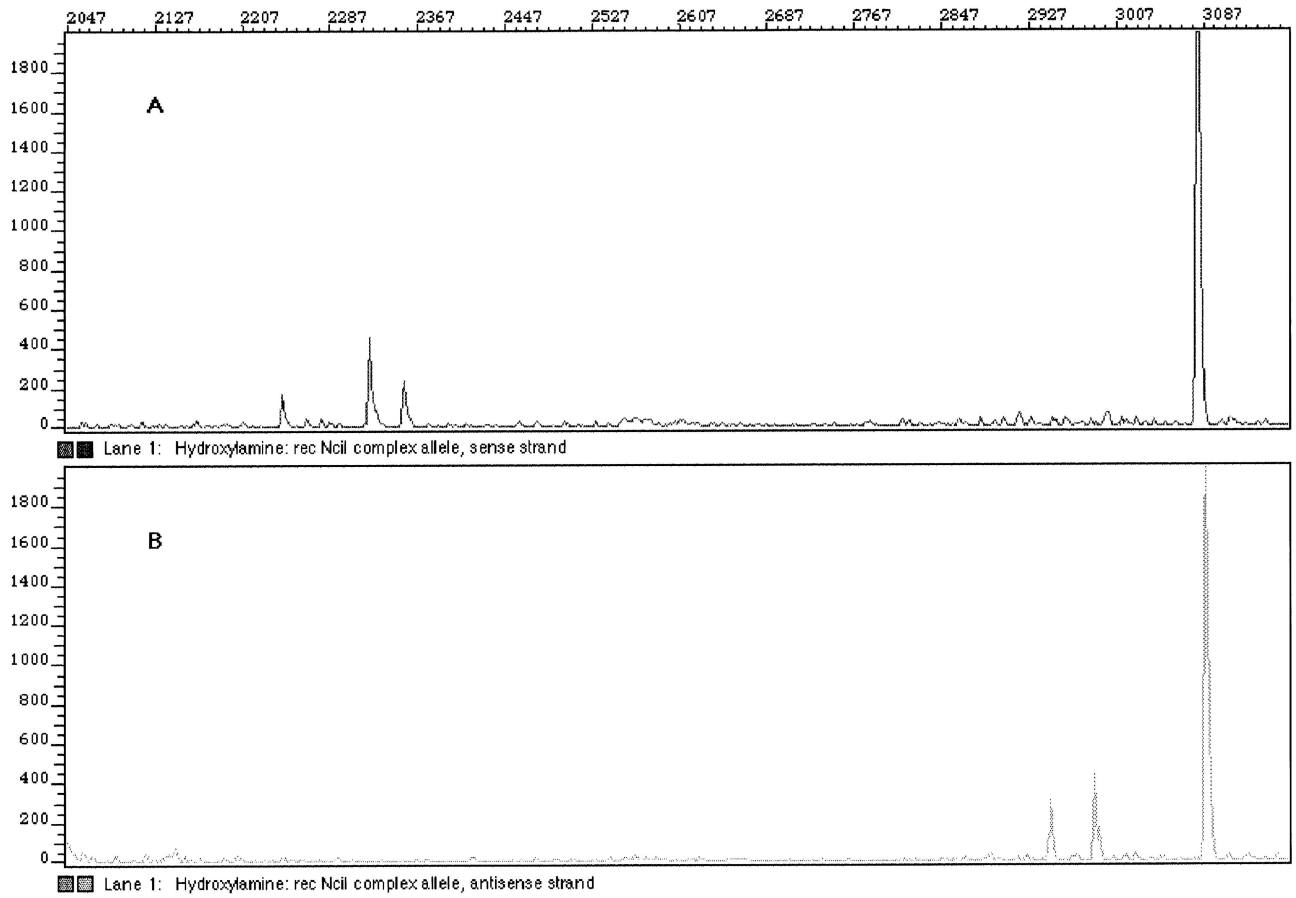


**Figure 4** Detection, by FAMA, of the complex allele rec NciI in a type 3 GD patient's gene. This complex allele consists of three single-base substitutions, all involving a cytosine. The L444P mutation (T→C transition) gives rise to C-A and T-G mismatches, whereas C-C and G-G heteroduplexes are formed at codons 456 and 460 (G→C transversion in both cases). C-A and C-C mismatches are detected by HA modification, whereas the T-G mismatch is revealed by osmium chemistry. G-G mismatches are not detectable. *A,* Electropherogram of sense strand, after HA modification (C specific), showing a high peak on the right, which corresponds to the uncleaved PCR amplicon (1,200 bp) encompassing exon 10, exon 11, and the 3′ UTR. Three additional cleavage peaks indicate the mispaired cytosines on the sense strand (C-A, C-C, and C-C mismatches). *B,* Fluorescence profile of antisense strand, after HA modification, revealing two additional cleavage peaks at complementary positions for codons 456 and 460, corresponding to cytosines on the antisense strand at both C-C heteroduplexes. This illustrates the duplication of information obtained, from the same gel, by differential end labeling. Because of the large size of the amplicon, a logarithmic scale for the horizontal axis was used for both panels. Osmium tetroxide reaction resulted in a sixth cleavage peak on the sense strand, revealing the mismatched thymine of the second heteroduplex (T-G), occurring at codon 444 (T→C transition) (not shown).

was detected in three unrelated patients and was always associated with the same haplotype (fig. 3). Interestingly, all three patients originated from Brittany, suggesting a possible founder effect and the usefulness of screening for R120W when studying Celtic populations (Ferec et al. 1992). Alternatively, since the mutation occurred at a CpG dinucleotide and also is the sequence of the pseudogene, it could be due to a recurrent mutational event (Choy et al. 1997).

A third group included eight novel mutations distributed throughout the gene (fig. 2). All but one were missense mutations. They seem to be functionally important, since (1) 5/7 of the substituted amino acids (I119, R170, N188, K303, and L324) are evolutionarily conserved in human and mouse acid $\beta$-glucosidase (O'Neill et al. 1989); (2) most of the changes are nonconservative, with three amino acid substitutions (R170P, N188K, and K303I) resulting in charge changes and four (R170P, S237P, L324P, and A446P) introducing the helix-disrupting proline residue; and (3), by use of this highly sensitive technique, no double mutants (Savov et al. 1995) have been found, other than the complex allele rec NciI (fig. 4). All these arguments support the view that these mutations are responsible for enzyme deficiency, which ideally should be confirmed by expression studies (Grace et al. 1997; Pasmanik-Chor et al. 1997). Since heterozygote detection based on enzyme assay is notoriously unreliable, such rare mutations are of par-

ticular value for genetic counseling of families; these mutations also could be frequent in, up to now, poorly studied populations. In addition, all elucidated mutants may prove to be useful for a better understanding of protein structure and functional activity. The acid β-glucosidase catalytic domain consists of an $(\alpha/\beta)_8$ barrel with conserved functional amino acids at the C-terminal ends of six of the eight strands constituting the β-barrel (Henrissat et al. 1995). Of note, the arginine at position 120 is located at the C-terminal end of the β2 strand and is considered to be crucial for the activation of the active-site nucleophile Glu340 (Miao et al. 1994; Durand et al. 1997).

Twelve polymorphisms of the *GBA* gene, which are distributed in the 5′ sequence and throughout the introns, had been detected previously. Analysis of a large number of patients disclosed only four haplotypes, revealing a strong linkage disequilibrium (Beutler et al. 1992). During our survey, a novel haplotype, in addition to the pathogenic mutations, was identified in two patients carrying different genotypes (table 4). This association analysis with polymorphic markers, made possible by the broad DNA-scanning window of FAMA, may provide new information for population genetics.

### *Genotype/Phenotype Correlations*

The genotype/phenotype relationship for all 25 patients is presented in table 2. On the basis of previous data and the present study, the following general considerations can be drawn. It appears that GD severity may be attenuated by the dominant influence of the N370S mild allele. Nevertheless, although the heteroallelic presence of N370S allows prediction of a nonneuronopathic clinical course (NIH Technology Assessment Panel on Gaucher Disease 1996), visceral involvement can be highly variable. The same N370S/R120W genotype was found in three patients who exhibited strikingly different phenotypes, thus underlining the phenotypic variation associated with identical genotypes among unrelated individuals (table 2). Other associations with the N370S allele (I119T, N188K, S237P, and L324P) were seen only once. The severity of these novel alleles, which may determine the individual clinical outcome, therefore cannot be assessed clearly and can only be speculated (table 2). However, it should be noted that hydrophobic cluster analysis predicts an important role for Ile119 and Ser237, within the catalytic site (Glu235 being the conserved proton donor) (Durand et al. 1997), in accordance with the severe clinical outcome associated with their substitution.

The severity of the common L444P was confirmed in our series, in which two children, homozygous for this latter mutation, exhibited type 3 GD (table 2), whereas another L444P/L444P homozygote case was found in an African neonate originating from Rwanda, who presented with type 2 GD and died at 18 mo of age (authors' unpublished data, not included in this French series). Interestingly, the complex allele rec NciI (L444P + A456P + V460V) was evidenced in patient 21 (fig. 4), who developed neurological symptoms typical of type 3 GD and who died despite enzyme recombinant therapy. His complete genotype was characterized as rec NciI/V394L, thus confirming that the V394L mutation obviously is severe (Beutler and Gelbart 1996).

It is certainly an oversimplification to determine the severity of a given missense mutation when only the amino acids involved in the substitution have been considered. The nature and location of the change must be considered in relation to the three-dimensional structure, the active site, or potentially important domains of the enzyme. The R48W mutation was observed in association with L444P, in patient 17. The nonconservative substitution of tryptophan for arginine, with loss of a positive charge and introduction of a more sterically rigid, bulky side chain, could be expected to be deleterious. Conversely, a functional approach recently has

**Table 4**

**Nucleotides at Six Polymorphic Sites in the Previously Known and the Novel Glucocerebrosidase Haplotypes**

| | Nucleotide, at Polymorphic Site[a] | | | | | |
|---|---|---|---|---|---|---|
| Haplotype | 2127 (Intron 4) [1545] | 2840 (Intron 4) [2251] | 3304 (Intron 5) (2714) | 3938 (Intron 6) [3348] | 5147 (Intron 7) [4552] | 6157 (Intron 9) [5561] |
| Plus (+)[b] | a | c | g | g | c | g |
| Minus (−)[b] | g | g | a | a | a | a |
| African[b] | g | a | a | a | a | a |
| Uncommon variant[b] | a | c | g | g | c | g |
| Pseudogene sequence | Del | g | g | Del | Del | a |
| Novel haplotype | a | g | a | a | c | g |

[a] Numbers within brackets indicate nucleotide numbering according to Beutler and Gelbart (1996). Del = deleted.

[b] Data from the report by Beutler et al. (1992).

demonstrated that the R48W mutation retains a significant residual enzymatic activity (Grace et al. 1997). Our clinical data agree with this study and favor the mild severity of the R48W allele.

In spite of the general relationship between the inherited mutations and the disease manifestations, unexplained discrepancies remain. Mutations alone seem unable to completely predict the phenotypic expression. A typical example is the severely affected 22-year-old woman (patient 25a) and her asymptomatic brother (patient 25b), who were shown to carry the same homozygous missense mutation, with homozygosity making the severity of the allele more relevant to study (table 2). Such a phenotypic variation of a simple Mendelian condition within kindreds emphasizes the influence of modulating factors. Possible mechanisms involved in or responsible for phenotypic variation in cases of identical pathogenic mutations may be multifactorial: they include additional intragenic sequence alterations, specific modifier genes (Rozmahel et al. 1996), and the genetic background in general, as well as the influence of the environment (Wolf 1997). In this respect, the identification of an additional *GBA* haplotype is interesting, since the severity of GD may be influenced by a different genetic background of the *GBA* gene. Indeed, the influence of otherwise neutral polymorphisms on pathogenic mutations recently has been suggested for cystic fibrosis (Cuppens et al. 1998).

Occurrence of clinical heterogeneity in sibs homozygous for identical pathogenic mutations is puzzling. It rules out additional intragenic sequence alterations, as has been suspected (Savov et al. 1995), but favors unlinked genetic or environmental factors. The role of a modifier gene(s) acting in *cis,* as has been proposed recently for flanking genes at the *GBA* locus (Winfield et al. 1997), or in *trans,* as suggested by the striking difference in phenotypic expression observed within families in our series, remains to be demonstrated formally in GD (Moran et al. 1997).

In accordance with data emerging for other Mendelian traits—such as craniosynostosis (Rutland et al. 1995), cystic fibrosis (Kiesewetter et al. 1993), and even sickle-cell disease, which is a paradigm for monogenic diseases (Serjeant 1997)—the role of multifactorial control is further emphasized here. Although it is the primary factor, the mutation does not explain the entire genotype/phenotype relationship. A disease phenotype corresponding to a particular mutation will remain unpredictable until a more efficient analysis of its genetic expression becomes routinely available; this should lead to caution in genetic counseling. Thus, the Mendelian concept of a monogenic trait or a monofactorial disease can no longer be regarded as absolute, since the influence of a multifactorial control on the realization of the phenotype is increasingly being recognized.

## Acknowledgments

The authors would like to thank the families and the clinicians for their help during this project. We gratefully acknowledge Jeanne Manicom and Emmanuel Gomas for their expert technical assistance; Dr. Mario Tosi for his advice and comments on the work while it was in progress; and Drs. Jamel Chelly, Fiona Francis, and Dominique Labie for their critical reading of the manuscript. This work was supported, in part, by grants from Vaincre les Maladies Lysosomales.

## Electronic-Database Information

Accession numbers and URLs for data in this article are as follows:

European Molecular Biology Laboratory, http://srs.ebi.ac.uk.5000/srs5bin/cgi-bin/wgetz

GenBank, http://www.ncbi.nlm.nih.gov/cgi-bin/genbank (for cDNA sequences [M11080] and for the acid $\beta$-glucosidase sequence [J03059])

Online Mendelian Inheritance in Man (OMIM), http://www.ncbi.nlm.nih.gov/Omim (for type 1 GD [MIM 230800], type 2 GD [MIM 230900], and type 3 GD [MIM 231000])

## References

Abrahamov A, Elstein D, Gross-Tsur V, Farber B, Glaser Y, Hadas-Halpern I, Ronen S, et al (1995) Gaucher's disease variant characterised by progressive calcification of heart valves and unique genotype. Lancet 346:1000–1003

Amaral O, Fortuna AM, Lacerda L, Pinto R, Sa Miranda MC (1994) Molecular characterisation of type 1 Gaucher disease families and patients: intrafamilial heterogeneity at the clinical level. J Med Genet 31:401–404

Beutler E, Gelbart T (1993) Gaucher disease mutations in non-Jewish patients. Br J Haematol 85:401–405

——— (1996) Glucocerebrosidase (Gaucher disease). Hum Mutat 8:207–213

Beutler E, Grabowski GA (1995) Glucosylceramide lipidoses: Gaucher disease. In: Scriver CR, Beaudet AL, Sly WS, Valle D (eds) The metabolic and molecular bases of inherited disease, 7th ed. McGraw-Hill, New York, pp 2641–2670

Beutler E, Nguyen NJ, Hennenberger MW, Smolec JM, McPherson RA, West C, Gelbart T (1993) Gaucher disease: gene frequencies in the Ashkenazi Jewish population. Am J Hum Genet 52:85–88

Beutler E, West C, Gelbart T (1992) Polymorphisms in the human glucocerebrosidase gene. Genomics 12:795–800

Boot RG, Hollak CE, Verhoek M, Sloof P, Poorthuis BJ, Kleijer WJ, Wevers RA, et al (1997) Glucocerebrosidase genotype of Gaucher patients in the Netherlands: limitations in prognostic value. Hum Mutat 10:348–358

Brady RO, Barton NW, Grabowski GA (1993) The role of neurogenetics in Gaucher disease. Arch Neurol 50: 1212–1224

Choy FY, Humphries ML, Shi H (1997) Identification of two novel and four uncommon missense mutations among Chinese Gaucher disease patients. Am J Med Genet 71:172–178

Cormand B, Vilageliu L, Burguera JM, Balcells S, Gonzalez-Duarte R, Grinberg D, Chabas A (1995) Gaucher disease in Spanish patients: analysis of eight mutations. Hum Mutat 5:303–309

Cotton RGH (1997) Slowly but surely towards better scanning for mutations. Trends Genet 13:43–46

Cotton RGH, Rodriguez NR, Campbell RD (1988) Reactivity of cytosine and thymine in single-base pair mismatched with hydroxylamine and osmium tetroxide and its application to the study of mutations. Proc Natl Acad Sci USA 85: 4397–4401

Cuppens H, Lin W, Jaspers M, Costes B, Teng H, Vankerberghen A, Jorissen M, et al (1998) Polyvariant mutant cystic fibrosis transmembrane conductance regulator genes. J Clin Invest 101:487–496

Daniels LB, Glew RH (1982) $\beta$-Glucosidase assays in the diagnosis of Gaucher's disease. Clin Chem 28:569–577

Dianzani I, Forrest SM, Camaschella C, Gottardi E, Cotton RGH (1991) Heterozygotes and homozygotes: discrimination by chemical cleavage of mismatch. Am J Hum Genet 48:423–424

Durand P, Lehn P, Callebaut I, Fabrega S, Henrissat B, Mornon JP (1997) Active-site motifs of lysosomal acid hydrolases: invariant features of clan GH-A glycocyl hydrolases deduced from hydrophobic cluster analysis. Glycobiology 7:277–284

Ferec C, Audrezet MP, Mercier B, Guillermit H, Moullier P, Quere I, Verlingue C (1992) Detection of over 98% cystic fibrosis mutations in a Celtic population. Nat Genet 1: 188–191

Germain D, Biasotto M, Tosi M, Meo T, Kahn A, Poenaru L (1996) Fluorescence-assisted mismatch analysis for exhaustive screening of the $\alpha$-galactosidase A gene and detection of carriers in Fabry disease. Hum Genet 98:719–726

Grabowski GA, Saal HM, Wenstrup RJ, Barton NW (1996) Gaucher disease: a prototype for molecular medicine. Crit Rev Oncol Hematol 23:25–55

Grace ME, Desnick RJ, Pastores GM (1997) Identification and expression of acid $\beta$-glucosidase mutations causing severe type 1 and neurologic type 2 Gaucher disease in non-Jewish patients. J Clin Invest 99:2530–2537

Griffais R, André PM, Thibon M (1991) K-tuple frequency in the human genome and polymerase chain reaction. Nucleic Acids Res 19:3887–3891

Grompe M (1993) The rapid detection of unknown mutations in nucleic acids. Nat Genet 5:111–117

He G-S, Grabowski GA (1992) Gaucher disease: a $G^{+1} \rightarrow A^{+1}$ IVS2 splice donor site mutation causing exon 2 skipping in the acid $\beta$-glucosidase mRNA. Am J Hum Genet 51: 810–820

Henrissat B, Callebaut I, Fabrega S, Lehn P, Mornon JP, Davies G (1995) Conserved catalytic machinery and the prediction of a common fold for several families of glycosyl hydrolases. Proc Natl Acad Sci USA 92:7090–7094

Horowitz M, Tzuri G, Eyal N, Berebi A, Kolodny EH, Brady RO, Barton NW, et al (1993) Prevalence of nine mutations among Jewish and non-Jewish Gaucher disease patients. Am J Hum Genet 53:921–930

Horowitz M, Wilder S, Horowitz Z, Reiner O, Gelbart T, Beutler E (1989) The human glucocerebrosidase gene and pseudogene: structure and evolution. Genomics 4:87–96

Ida H, Iwasawa K, Kawame H, Rennert OM, Maekawa K, Eto Y (1995) Characteristics of gene mutations among 32 unrelated Japanese Gaucher disease patients: absence of the common Jewish 84GG and 1226G mutations. Hum Genet 95:717–720

Kiesewetter S, Macek M Jr, Davis C, Curristin SM, Chu CS, Graham C, Shrimpton AE, et al (1993) A mutation in CFTR produces different phenotypes depending on chromosomal background. Nat Genet 5:274–278

Kwok PY, Carlson C, Yager TD, Ankener W, Nickerson DA (1994) Comparative analysis of human DNA variations by fluorescence-based sequencing of PCR products. Genomics 23:138–144

Latham T, Grabowski GA, Theophilus BDM, Smith FI (1990) Complex alleles of the acid $\beta$-glucosidase gene in Gaucher disease. Am J Hum Genet 47:79–86

Latham TE, Theophilus BDM, Grabowski GA, Smith FI (1991) Heterogeneity of mutations in the acid $\beta$-glucosidase gene in Gaucher disease patients. DNA Cell Biol 10:15–21

Le Coutre P, Demina A, Beutler E, Beck M, Petrides P (1997) Molecular analysis of Gaucher disease: distribution of eight mutations and the complete gene deletion in 27 patients from Germany. Hum Genet 99:816–821

Miao S, McCarter JD, Grace ME, Grabowski GA, Aebersold R, Withers SG (1994) Identification of Glu340 as the active-site nucleophile in human glucocerebrosidase by use of electrospray tandem mass spectrometry. J Biol Chem 269: 10975–10978

Moran D, Galperin E, Horowitz M (1997) Identification of factors regulating the expression of the human glucocerebrosidase gene. Gene 194:201–213

NIH Technology Assessment Panel on Gaucher Disease (1996) Gaucher disease: current issues in diagnosis and treatment. JAMA 275:548–553

O'Neill RR, Tokoro T, Kozak CA, Brady RO (1989) Comparison of the chromosomal localization of murine and human glucocerebrosidase genes and of the deduced amino acid sequences. Proc Natl Acad Sci USA 86:5049–5053

Pasmanik-Chor M, Madar-Shapiro L, Stein OE, Aerts H, Gatt S, Horowitz M (1997) Expression of mutated glucocerebrosidase alleles in human cells. Hum Mol Genet 6:887–895

Phelps RS, Chadwick RB, Conrad MP, Kronick MN, Kamb A (1995) Efficient, automatic detection of heterozygous bases during large-scale DNA sequence screening. Biotechniques 19:984–989

Rowley G, Saad S, Gianelli F, Green PM (1995) Ultrarapid mutation detection by multiplex, solid-phase chemical cleavage. Genomics 30:574–582

Rozmahel R, Wilschanski M, Matin A, Plyte S, Oliver M, Auerbach W, Moore A, et al (1996) Modulation of disease severity in cystic fibrosis transmembrane conductance regulator deficient mice by a secondary genetic factor. Nat Genet 12:280–287

Rutland P, Pulleyn LJ, Reardon W, Baraitser M, Hayward R, Jones B, Malcolm S, et al (1995) Identical mutations in the FGFR2 gene cause both Pfeiffer and Crouzon syndrome phenotypes. Nat Genet 9:173–176

Savov A, Angelicheva D, Balassopoulou A, Jordanova A, Noussia-Arvanitakis S, Kalaydjieva L (1995) Double mutant alleles: are they rare? Hum Mol Genet 4:1169–1171

Serjeant GR (1997) Sickle cell disease. Lancet 350:725–730
Sibille A, Eng CM, Kim S-J, Pastores G, Grabowski GA (1993) Phenotype/genotype correlations in Gaucher disease type I: clinical and therapeutic implications. Am J Hum Genet 52: 1094–1101
Sidransky E, Ginns E (1993) Clinical heterogeneity among patients with Gaucher's disease. JAMA 269:1154–1157
Sorje J, West C, Westwood B, Beutler E (1985) Molecular cloning and nucleotide sequence of human glucocerebrosidase gene. Proc Natl Acad Sci USA 82:7289–7293
Tayebi N, Cushner S, Sidransky E (1996) Differentiation of the glucocerebrosidase gene from pseudogene by long-template PCR: implications for Gaucher disease. Am J Hum Genet 59:740–741
Verpy E, Biasotto M, Brai M, Misiano G, Meo T, Tosi M (1996) Exhaustive mutation scanning by fluorescence-assisted mismatch analysis discloses new genotype-phenotype correlations in angioedema. Am J Hum Genet 59:308–319
Verpy E, Biasotto M, Meo T, Tosi M (1994) Efficient detection of point mutations on color-coded strands of target DNA. Proc Natl Acad Sci USA 91:1873–1877
Winfield SL, Tayebi N, Martin BM, Ginns EI, Sidransky E (1997) Identification of three additional genes contiguous to the glucocerebrosidase locus on chromosome 1q21: implications for Gaucher disease. Genome Res 7:1020–1026
Wolf U (1997) Identical mutations and phenotypic variation. Hum Genet 100:305–321
Zimran A, Elstein D, Abrahamov A, Kuhl W, Brown KH, Beutler E (1995) Prenatal molecular diagnosis of Gaucher disease. Prenat Diagn 15:1185–1188